Electronic Supplementary Material (ESI) for Chemical Communications.

Electronic Supplementary Information

Linear conjugated polymer photocatalysts with varied linker units for photocatalytic hydrogen evolution from water

Lunjie Liu,[a] Michał A. Kochman,[b] Wei Zhao,[a] Martijn A. Zwijnenburg,*[b] and Reiner Sebastian Sprick*[c]

[a] Department of Chemistry and Materials Innovation Factory, University of Liverpool, 51 Oxford Street, Liverpool L7 3NY, UK.

[b] Department of Chemistry, University College London, 20 Gordon Street, London WC1H 0AJ, UK.

[c] Department of Pure and Applied Chemistry, University of Strathclyde, Thomas Graham Building, 295 Cathedral Street, Glasgow G1 1XL, UK.

* Corresponding authors: m.zwijnenburg@ucl.ac.uk (M.A.Z.), sebastian.sprick@strath.ac.uk (R.S.S.).

1 Materials

All reagents were obtained from Sigma-Aldrich, Fluorochem, TCI or Alfa Aesar and used as received.

2 Experiment methods

2.1 General characterization

The absorption spectra of the polymers were measured on a Cary 5000 UV-visible-NIR spectrophotometer in solid powder state. Transmission FT-IR spectra were collected with an attenuated total reflectance (ATR) method on a Bruker Tensor-27 spectrometer for 16 scans with a resolution of 4 cm^{-1} at room temperature. Photoluminescence spectra were performed on a Shimadzu RF-5301PC fluorescence spectrometer. Time-correlated single photon counting (TCSPC) experiments were measured on an Edinburgh Instruments LS980-D2S2-STM spectrometer (EPL-375 diode, λ = 371 nm) equipped with picosecond pulsed LED excitation sources and a R928 detector, with a stop count rate below 5%. The instrument response of the TCSPC spectrometer was measured with colloidal silica (LUDOX HS-40, Sigma-Aldrich) at the excitation wavelength. Decay times were fitted in the FAST software using three decay exponents. Samples were prepared by ultrasonicating the polymer in water. Thermogravimetric analysis was performed by heating samples under N_2 in open platinum pans from 25 °C to 800 °C at 10 °C min^{-1} on an EXSTAR6000 instrument. PXRD measurements were performed on a Panalytical Empyrean diffractometer with a Cu X-ray source (λ = 1.5418 Å, Cu Kα), polymers were placed on an aluminium well plate and screened in high throughput transmission mode with PIXCEL 3D detector and X-ray focusing mirror. Static light scattering measurements were performed on a Malvern Mastersizer 3000 Particle Sizer at a laser obscuration of 5-10%. Particle sizes were fitted according to the Mie theory with the Malvern 'General Purpose' analysis model. Transmittance of high-throughput samples was measured on a Formulaction S.A.S. Turbiscan AGS system with an 880 nm NIR diode and a detector at 180° (relative to the light source) in a cylindrical glass cell. Surface areas were tested on Micromeritics 2420 instrument at a temperature of 77 K. Before analysis, polymer samples were degassed offline at 110 °C for 15 hours under dynamic vacuum (10^{-5} bar). CHNS-O Analyzer was measured using standard microanalytical procedures. Palladium contents were determined using ICP-OES Agilent 5110 equipped with a collision/reaction cell after a microwave digestion of the materials in nitric acid (67-69%, trace metal analysis grade) in the instrument of Perkin Elmer Microwave Titan. Water contact angles were measured using pressed pellets and a drop-shape analysis apparatus (Krüss DSA100) with the Young-Laplace fitting method. The morphology of the polymer was studied on a Hitachi S4800 scanning electron microscope (SEM).

2.2 Synthesis of polymers

General procedure for Suzuki-Miyaura polycondensation: A flask was charged with the monomers, toluene and an aqueous solution of K_2CO_3 (2.0 M) and after degassed by bubbling with N_2 for 30 min, $[Pd(PPh_3)_4]$ was added and degassed additional 15 minutes. The reaction mixture was heated to 110 °C and kept at this temperature for 3 days. After cooled to room temperature, the mixture was poured into methanol, and filtered off. The precipitate was further purified by Soxhlet extraction with methanol and chloroform. The final product was dried in the vacuum oven at 80 °C overnight.

LS1: 3,7-Bis(4,4,5,5-tetramethyl-1,3,2-dioxaborolan-2-yl)dibenzo[*b*,*d*]thiophene sulfone (468 mg, 1 mmol), 1,2-bis(4-bromophenyl)ethane (340 mg, 1 mmol), $[Pd(PPh_3)_4]$ (18 mg), 18 mL toluene and 8 mL K_2CO_3 aqueous solution (2.0 M) were used in this polymerization. After work-up and Soxhlet the product was obtained as a grey powder (229.8 mg, 58%). Anal. Calcd for $(C_{12}H_4S)_n$: C, 79.16; H, 4.60; S, 8.13%; Found C, 73.13; H, 4.52; S, 7.56%. Pd content: 0.54%.

LS2: 3,7-Bis(4,4,5,5-tetramethyl-1,3,2-dioxaborolan-2-yl)dibenzo[*b*,*d*]thiophene sulfone (468 mg, 1 mmol), *trans*-4,4'-dibromostilbene (338 mg, 1 mmol), $[Pd(PPh_3)_4]$ (18 mg), 18 mL toluene and 8 mL K_2CO_3 aqueous solution (2.0 M) were used in this polymerization. After work-up and Soxhlet the product was obtained as a green powder (262.7 mg, 67%). Anal. Calcd for $(C_{12}H_4S)_n$: C, 79.57; H, 4.11; S, 8.17%; Found C, 71.16; H, 4.11; S, 6.85%. Pd content: 0.40%.

LS3: 3,7-Bis(4,4,5,5-tetramethyl-1,3,2-dioxaborolan-2-yl)dibenzo[*b*,*d*]thiophene sulfone (468 mg, 1 mmol), bis(4-bromophenyl)acetylene (336 mg, 1 mmol), $[Pd(PPh_3)_4]$ (18 mg), 18 mL toluene and 8 mL K_2CO_3 aqueous solution (2.0 M) were used in this polymerization. After work-up and Soxhlet the product was obtained as a yellow powder (335.9 mg, 86%). Anal. Calcd for $(C_{12}H_4S)_n$: C, 79.98; H, 3.61; S, 8.21%; Found C, 71.23; H, 3.58; S, 8.13%. Pd content: 0.45%.

LF1: 9,9-Dimethyl-9*H*-fluorene-2,7-diboronic acid bis(pinacol) ester (446 mg, 1 mmol), 1,2-bis(4-bromophenyl)ethane (340 mg, 1 mmol), [Pd(PPh_3)$_4$] (18 mg), 18 mL toluene and 8 mL K_2CO_3 aqueous solution (2.0 M) were used in this polymerization. After work-up and Soxhlet the product was obtained as a grey powder (245.6 mg, 66%). Anal. Calcd for $(C_{12}H_4S)_n$: C, 93.51; H, 6.49%; Found C, 87.14; H, 6.14%. Pd content: 0.75%.

LF2: 9,9-Dimethyl-9*H*-fluorene-2,7-diboronic acid bis(pinacol) ester (446 mg, 1 mmol), *trans*-4,4'-dibromostilbene (338 mg, 1 mmol), [Pd(PPh_3)$_4$] (18 mg), 18 mL toluene and 8 mL K_2CO_3 aqueous solution (2.0 M) were used in this polymerization. After work-up and Soxhlet the product was obtained as a green powder (229.6 mg, 62%). Anal. Calcd for $(C_{12}H_4S)_n$: C, 94.01; H, 5.99%; Found C, 84.74; H, 5.57%. Pd content: 0.31%.

LF3: 9,9-Dimethy-9*H*-lfluorene-2,7-diboronic acid bis(pinacol) ester (446 mg, 1 mmol), bis(4-bromophenyl)acetylene (336 mg, 1 mmol), [Pd(PPh_3)$_4$] (18 mg), 18 mL toluene and 8 mL K_2CO_3 aqueous solution (2.0 M) were used in this polymerization. After work-up and Soxhlet the product was obtained as a green powder (193.6 mg, 53%). Anal. Calcd for $(C_{12}H_4S)_n$: C, 94.53; H, 5.47%; Found C, 82.19; H, 4.97%. Pd content: 0.60%.

2.3 Photocatalytic hydrogen evolution measurements

A quartz reaction flask was charged with 25 mg polymer and 25 mL mixture of water/methanol/triethylamine (1:1:1), the flask was sealed with a rubber septum. After ultrasonication for 10 minutes, the well-dispersed suspension was degassed by bubbling with N_2 for 30 minutes before illuminating with a 300 W Newport Xe light source with a 420 nm cut-off filter. The concentration of hydrogen was determined by a Bruker 450-GC gas chromatograph equipped with TCD detector. For longer-term stability experiments the polymer was recovered by filtration after illumination for 5 hours. After drying, 25 mL water/methanol/triethylamine (1:1:1) mixture was added again before the next run. External quantum efficiency (EQE) was estimated using the following formula:

$$EQE\% = \frac{2 \times Number\ of\ evolved\ H_2\ molecules}{Number\ of\ incident\ photons} \times 100\%$$

Experiments were performed under a light-emitting diode irradiation (λ = 420, 490, 700 nm).

2.4 Density functional theory (DFT) calculations

2.4.1 Conformation search

The structures of the oligomers were constructed with the program STK.[1] Afterwards, for each oligomer, we generated a set of 500 trial structures to serve as the starting points for the conformation search. These were sampled from molecular dynamics (MD) trajectories in which the electronic structure of the oligomer was treated with the use of the extended semiempirical tight-binding[2] (xTB) model. To allow the oligomer to sample a broad volume of the conformation space, during the MD simulations the temperature of the system was maintained at 600 K. Afterwards, the trial structures were optimised using xTB.

The resulting equilibrium geometries were ranked according to energy. It was assumed that the lowest-energy conformer of each oligomer is representative of the properties of the given polymer. Accordingly, this conformer was selected for the calculation of the electronic and optical properties.

In the case of oligomers LF1 and LS1, it was found that the low-energy conformers are those where the oligomer chain adopts a coiled, globule-like conformation. In order to gauge the effect of conformation on the optical and electronic properties of these oligomers, we additionally took into account some representative linear conformers. It is expected that in polymeric solids, where there are other polymer chains to interact with the geometry of the polymer chains will lie in between the coiled and linear conformations.

The xTB calculations were performed with the Semiempirical Extended Tight-Binding Program Package (xtb2019), version 5.6.4SE, and used the GFN_2 parameterization of the xTB model.[3] Aqueous solvation was represented via the generalised Born model augmented with the hydrophobic solvent accessible surface area term (GBSA). At the stage of the conformation search, all oligomers were considered to exist in the charge-neutral forms.

2.4.2 Calculation of optical and electronic properties

Having identified the representative conformer of each oligomer, we proceeded to optimize its geometry at the density functional theory (DFT) level. To calculate the adiabatic ionization potential (IP) and adiabatic electron affinity (EA) of the oligomer, the geometries of the radical cation and radical anion forms of the representative conformer were likewise optimized at the DFT level. Lastly, the excitation spectrum of the charge-neutral form of the representative conformer was calculated at the time-dependent DFT (TD-DFT) level of theory. For each polymer, the excited-state IP and EA values (denoted IP* and EA*, respectively) were calculated basing on of the vertical energy of the lowest singlet excited state (S_1).

The DFT and TD-DFT calculations were performed with the program Turbomole, version 6.5. The B3LYP exchange-correlation functional[4, 5] was used in combination with the DZP basis set.[6, 7] The effects of aqueous solvation were included via the conductor-like screening model[8, 9] (COSMO). At all times, the energies and gradients were corrected for dispersion effects with the D3 semiempirical dispersion correction scheme of Grimme and coworkers.[10]

3 Supporting figures and tables

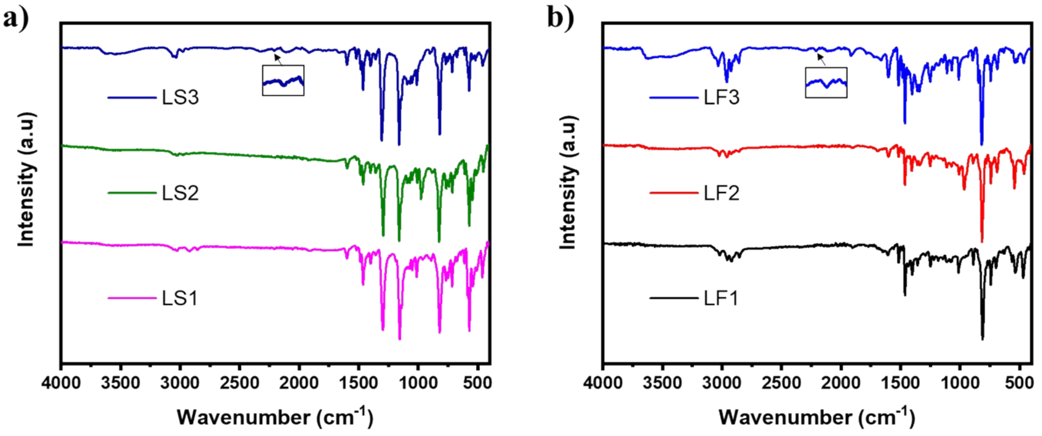

Fig. S1: Fourier-transform infrared spectra of a) LS1-3 and b) LF1-3.

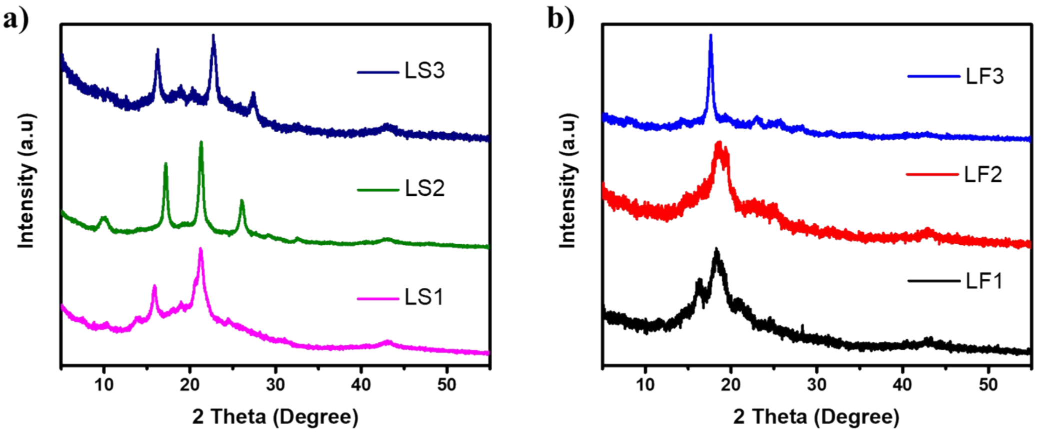

Fig. S2: PXRD patterns of a) LS1-3 and b) LF1-3.

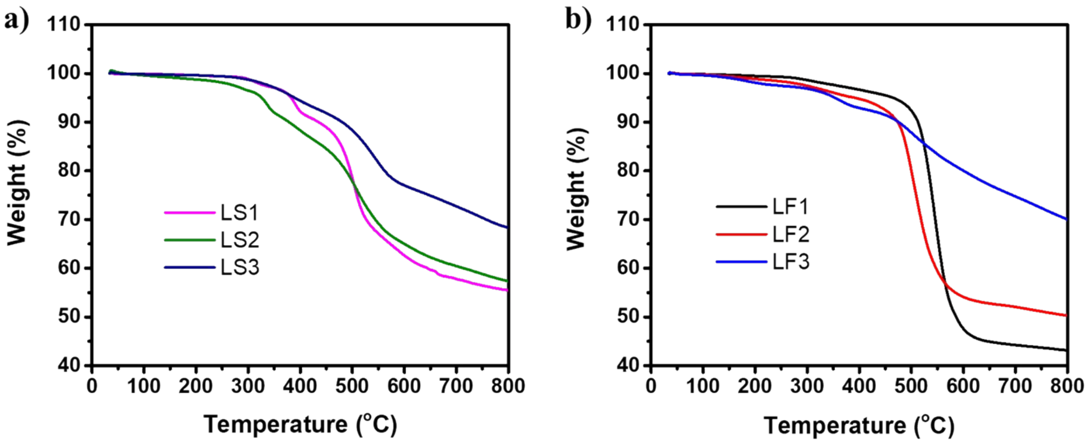

Fig. S3: Thermogravimetric analysis traces under N_2 of a) LS1-3 and b) LF1-3.

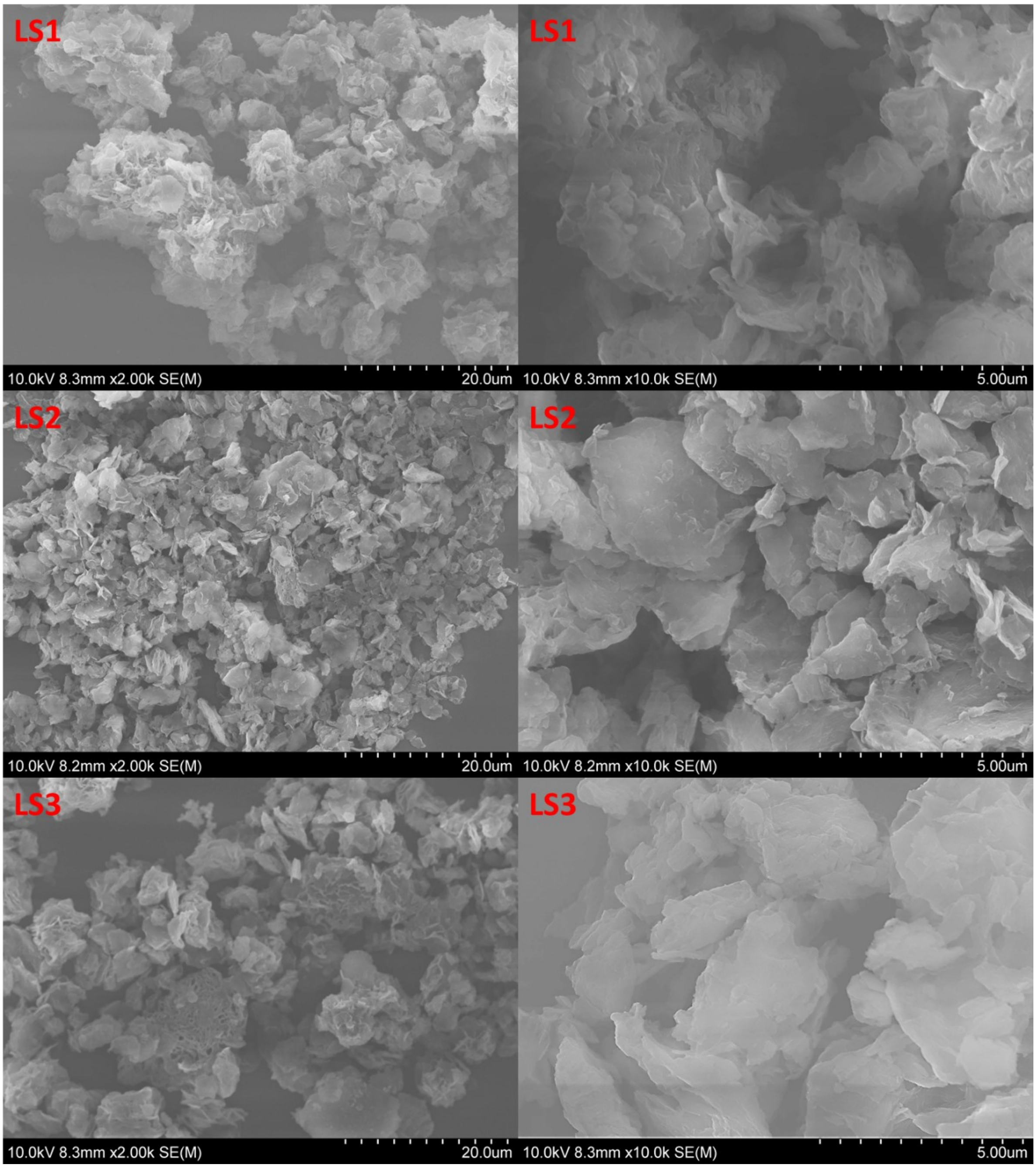

Fig. S4: Low magnification (Left) and high magnification (Right) SEM images of LS1-3.

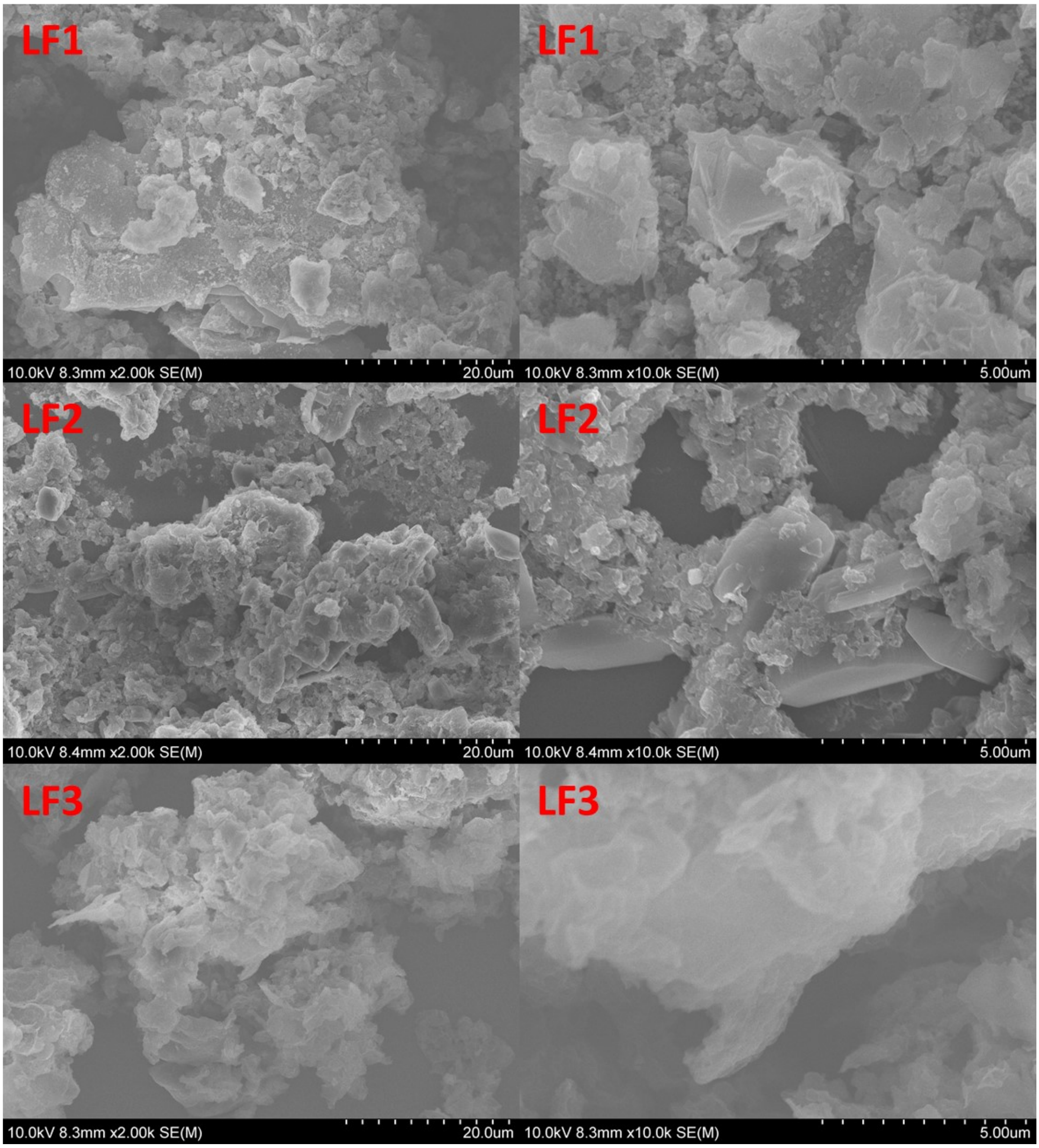

Fig. S5: Low magnification (Left) and high magnification (Right) SEM images of LF1-3.

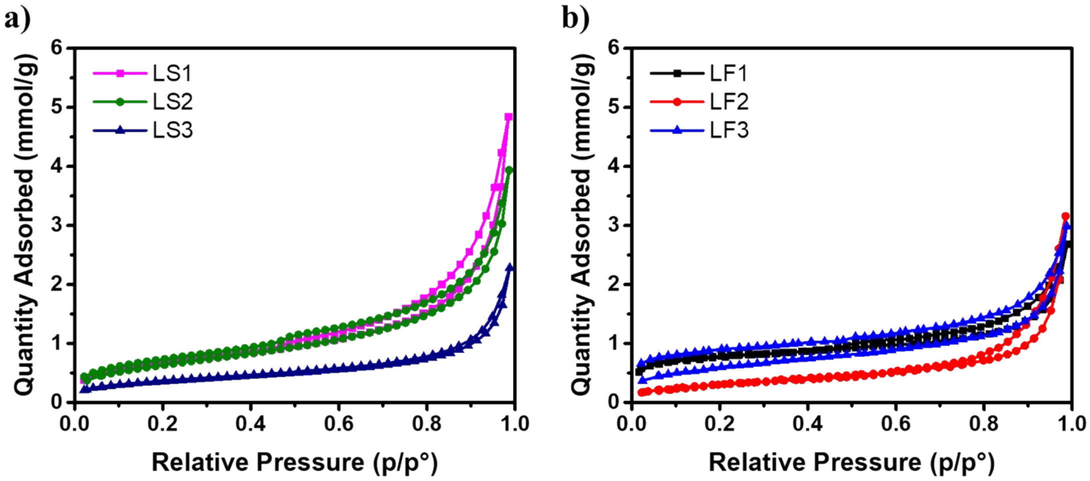

Fig. S6: Nitrogen sorption isotherm of LS1-3 and LF1-3.

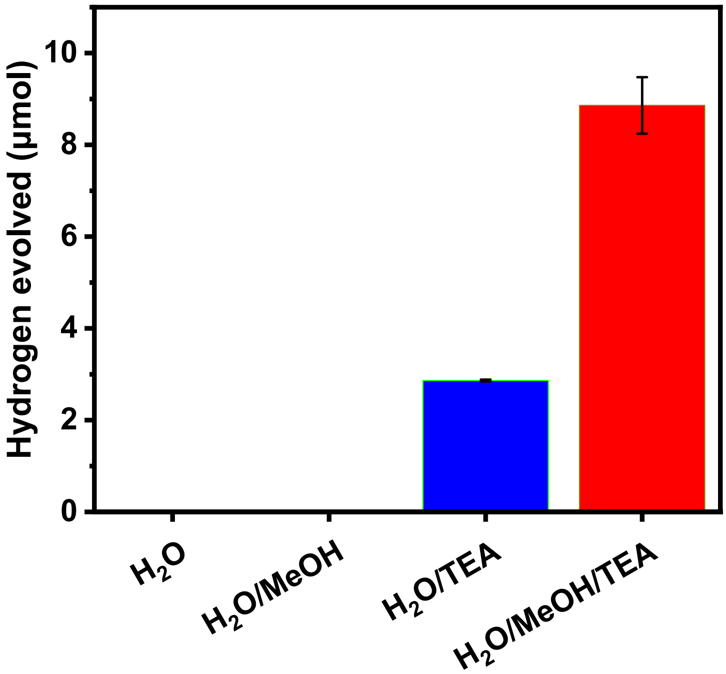

Fig. S7: Photocatalytic hydrogen production of LS2 in different reaction solutions: H_2O, H_2O/MeOH (1:1), H_2O/TEA (1:1), H_2O/MeOH/TEA (1:1:1). Experimental conditions: 2 mg LS2 in 5 mL solution was irradiated by an Oriel 94123A solar simulator with an output of 1.0 sun for 0.25 hour.

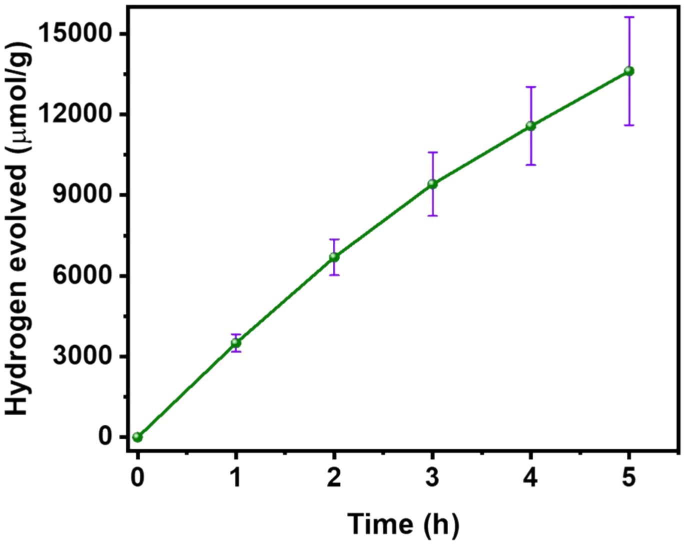

Fig. S8: Mean-variance three repeat runs of photocatalytic hydrogen evolution of photocatalyst LS2. Experimental conditions: 25 mg of the polymer photocatalyst in a H_2O/MeOH/TEA (1:1:1, 25 mL) solution was irradiated by a 300 W Xe light source with a $\lambda > 420$ nm cut-off filter.

Table S1: B3LYP predicted IP, EA, IP* and EA* values for the different polymers. For the alkyl polymers, LF1 and LS1, where the lowest energy conformer is coiled, potentials for both the lowest energy coiled conformer (coiled) and the lower linear non-coiled conformer (linear) are given.

Polymer	**IP / V**	**EA / V**	**IP* / V**	**EA* / V**
LS1 (linear)	1.264	-2.028	-2.096	1.331
LS1 (coiled)	0.857	-2.022	-2.312	1.147
LS2 (linear)	0.870	-1.794	-1.768	0.844
LS3 (linear)	1.081	-1.765	-1.735	1.052
LF1 (linear)	0.813	-2.530	-2.733	1.017
LF1 (coiled)	0.777	-2.704	-2.732	0.806
LF2 (linear)	0.622	-2.147	-2.103	0.578
LF3 (linear)	0.783	-2.144	-2.107	0.747

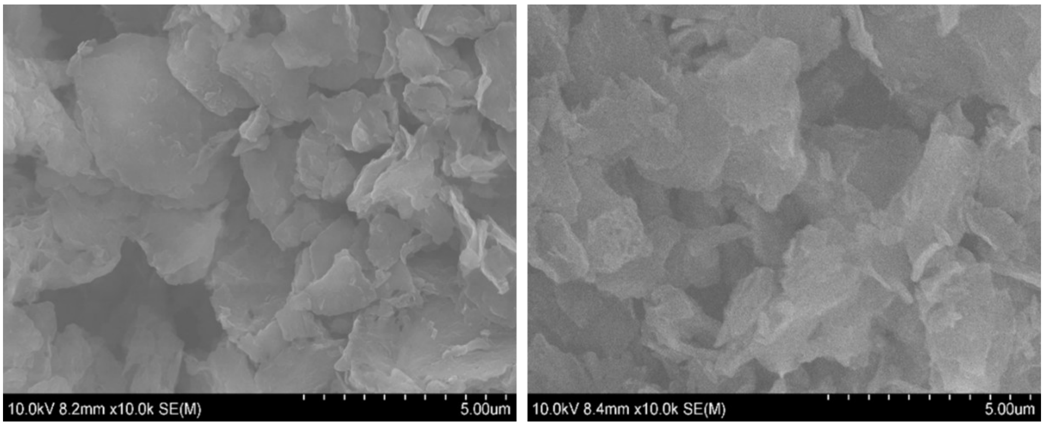

Fig. S9: SEM images of LS2 before (Left) and after (Right) long-term photocatalytic hydrogen evolution experiment.

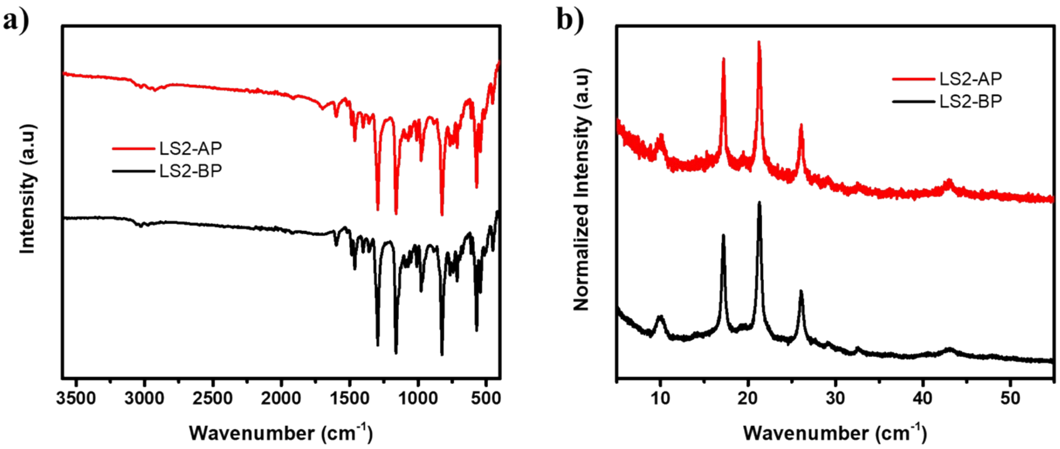

Fig. S10: a) FT-IR spectrum and b) PXRD patter of LS2 before (BP) and after (AP) long-term photocatalytic hydrogen evolution experiment.

Table S2: Comparation of LS2 with recent representative organic polymer photocatalysts for photocatalytic H_2 evolution.

Sample	Co-catalyst	Reaction solution[a]	λ / nm	EQE / %	Ref.
LS2	Residual Pd	TEA/MeOH/H_2O	420	5.6	**This work**
LS3	Residual Pd	TEA/MeOH/H_2O	420	4.6	**This work**
LS1	Residual Pd	TEA/MeOH/H_2O	420	3.9	**This work**
P64	Residual Pd	TEA/MeOH/H_2O	420	20.7	[11]
P10	Residual Pd	TEA/MeOH/H_2O	420	11.6	[12]
S-CMP3	Residual Pd	TEA/MeOH/H_2O	420	13.2	[13]
CTF-2	3 wt.% Pt	TEA/MeOH/H_2O	420	1.6	[14]
Pt/B-BT-1,4	3 wt.% Pt	TEOA/H_2O	420	4.01	[15]
OB-POP-3	3 wt.% Pt	TEOA/H_2O	420	2.0	[16]
PyBS-3	~3 wt.% Pt	AA/H_2O	420	29.3	[17]
PCP_{4e}	2 wt.% Pt	TEA/H_2O	350	1.8	[18]
g-C_3N_4/Ni_2P	-	TEOA/H_2O	435	3.2	[19]

[a] TEA: triethylamine, MeOH: methanol, TEOA: triethanolamine, AA: ascorbic acid.

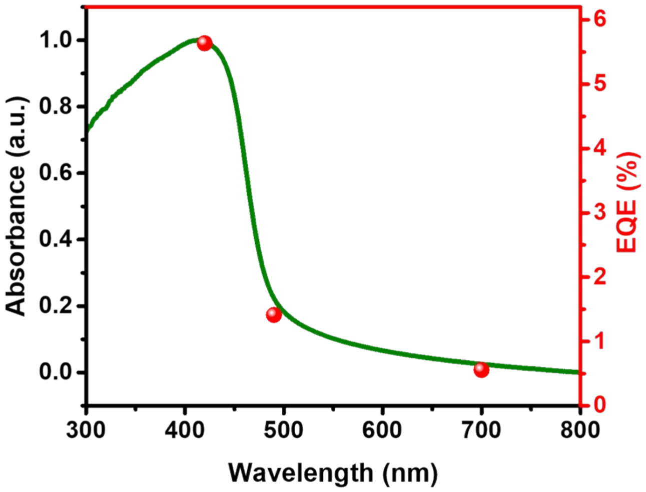

Fig. S11: Wavelength dependent external quantum efficiency (EQE) values and solid UV-vis spectrum of LS2, λ = 420, 490, 700 nm.

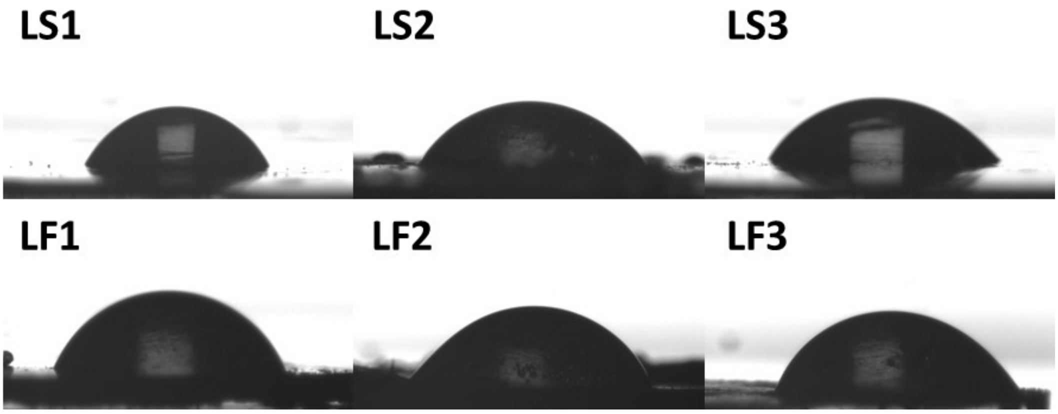

Fig. S12: Contact angle images against water of LS1-3 and LF1-3 measured as pallets.

Table S3: Particle sizes measured by static light scattering technique.

Polymer	**D_x50[a] / µm**	**$D[4,3]$[b] / µm**	**$D[3,2]$[c] / µm**	**Relative external surface area[d] / m^2 kg^{-1}**
LS1	14.0	15.7	7.9	763.7
LS2	11.4	13.6	6.1	987.3
LS3	15.1	18.0	9.5	633.2
LF1	20.1	23.2	8.7	686.2
LF2	20.3	24.4	8.1	745.1
LF3	18.6	19.7	10.6	565.5

[a] 50th percentile of particle size volume distribution; [b] Volume mean diameter; [c] Surface area mean diameter (Sauter mean diameter);[20] [d] Relative extrinsic surface area calculated by dividing the total surface area of the particles by the total mass, assuming a density of 1 g cm^{-3}.

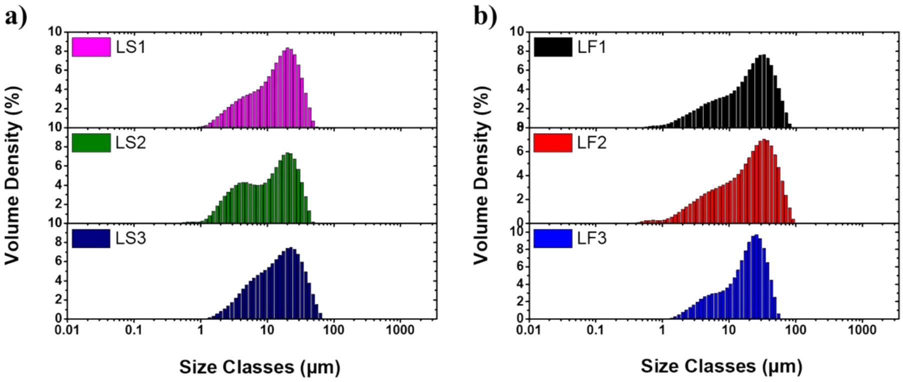

Fig. S13: Static light scattering experiments of a) LS1-3 and b) LF1-3 dispersed in water.

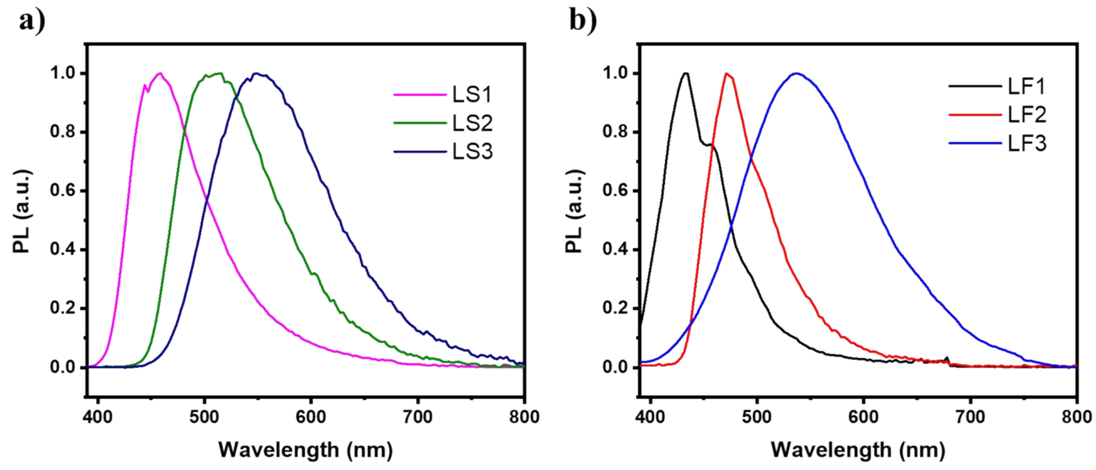

Fig. S14: Photoluminescence emission spectra of LS1-3 and LF1-3 (λ_{exc} = 371 nm).

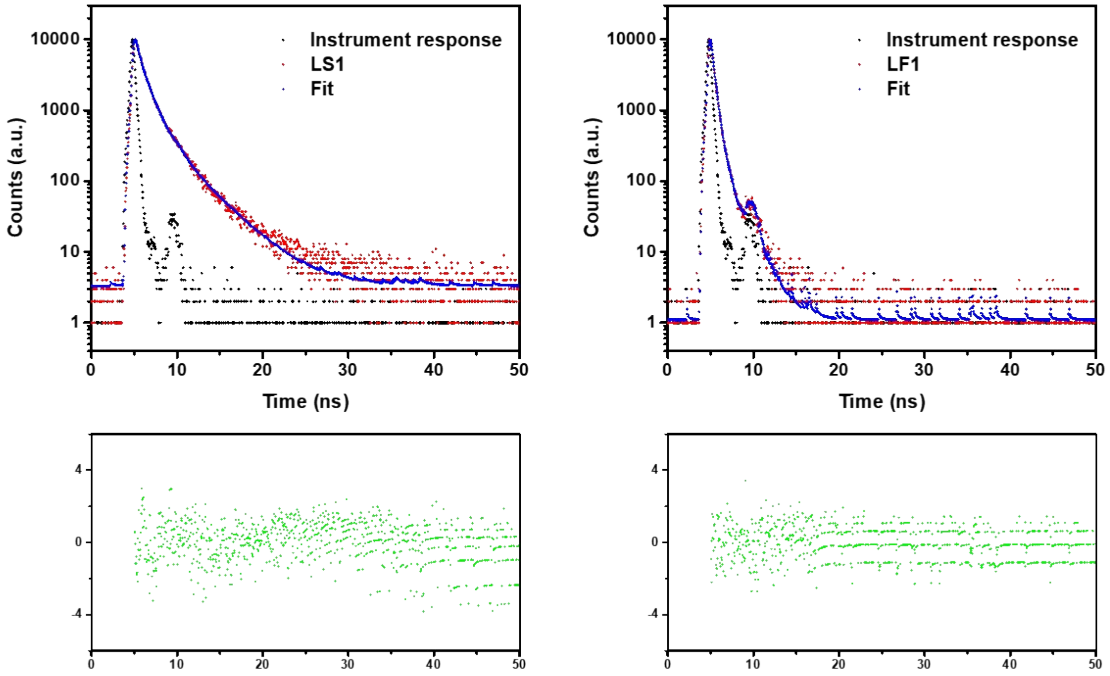

Fig. S15: Fluorescence life-time decays (top) and residuals (bottom) of LS1 and LF1.

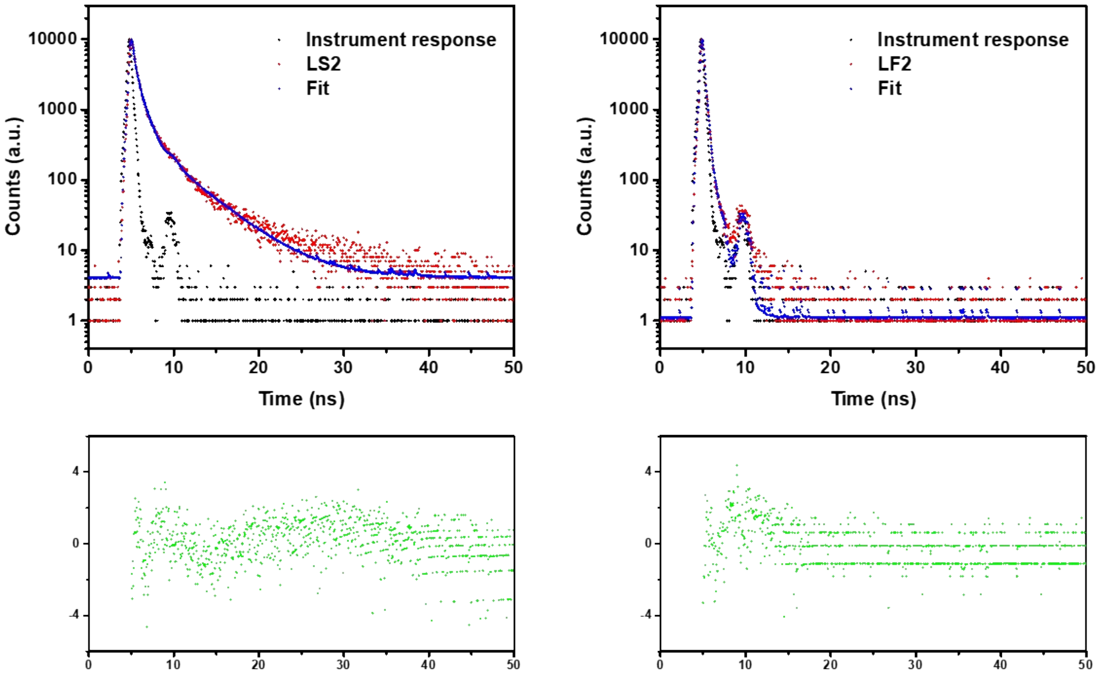

Fig. S16: Fluorescence life-time decays (top) and residuals (bottom) of LS2 and LF2.

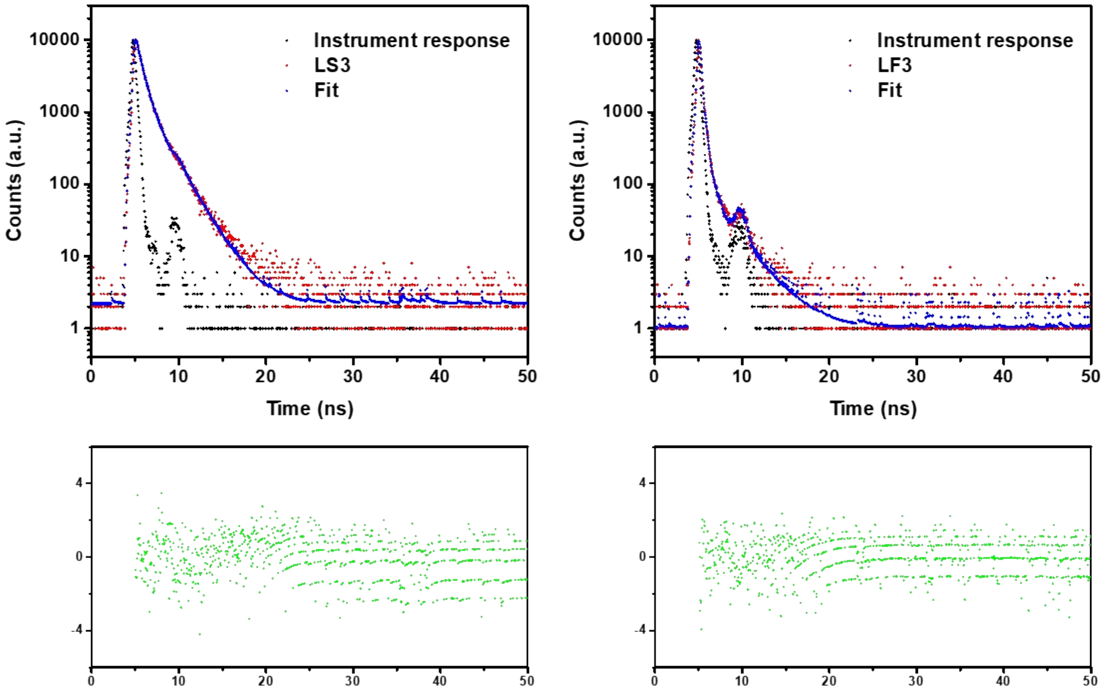

Fig. S17: Fluorescence life-time decays (top) and residuals (bottom) of LS3 and LF3.

Table S4: Estimated fluorescence lifetimes of LS1-3 and LF1-3.

Polymer	$\lambda_{\text{em-max}}$ / nm	τ_1 / ns	B_1 / %	τ_2 / ns	B_2 / %	τ_3 / ns	B_3 / %	χ^2	τ_{avg} / ns
LS1	460	0.50	37.14	1.43	51.12	4.39	11.74	1.23	1.43
LS2	510	0.36	53.24	1.60	35.18	7.06	11.58	1.53	1.57
LS3	550	0.38	37.10	1.08	49.68	2.75	13.22	1.26	1.04
LF1	430	0.09	60.92	0.49	35.21	1.82	3.87	0.81	0.30
LF2	475	0.09	39.46	0.10	54.90	0.69	5.65	1.07	0.13
LF3	540	0.07	82.70	0.42	14.47	2.64	2.83	0.95	0.19

[a] Fluorescence lifetimes for all polymers obtained from fitting time-correlated single photon counting decays to a sum of three exponentials, which yield τ_1, τ_2, and τ_3 according $\sum_{i=1}^{n}\left(A + B_i exp(-t/\tau_i)\right)$. τ_{avg} is the weighted average lifetime calculated as $\sum_{i=1}^{n}(B_i\tau_i)$.

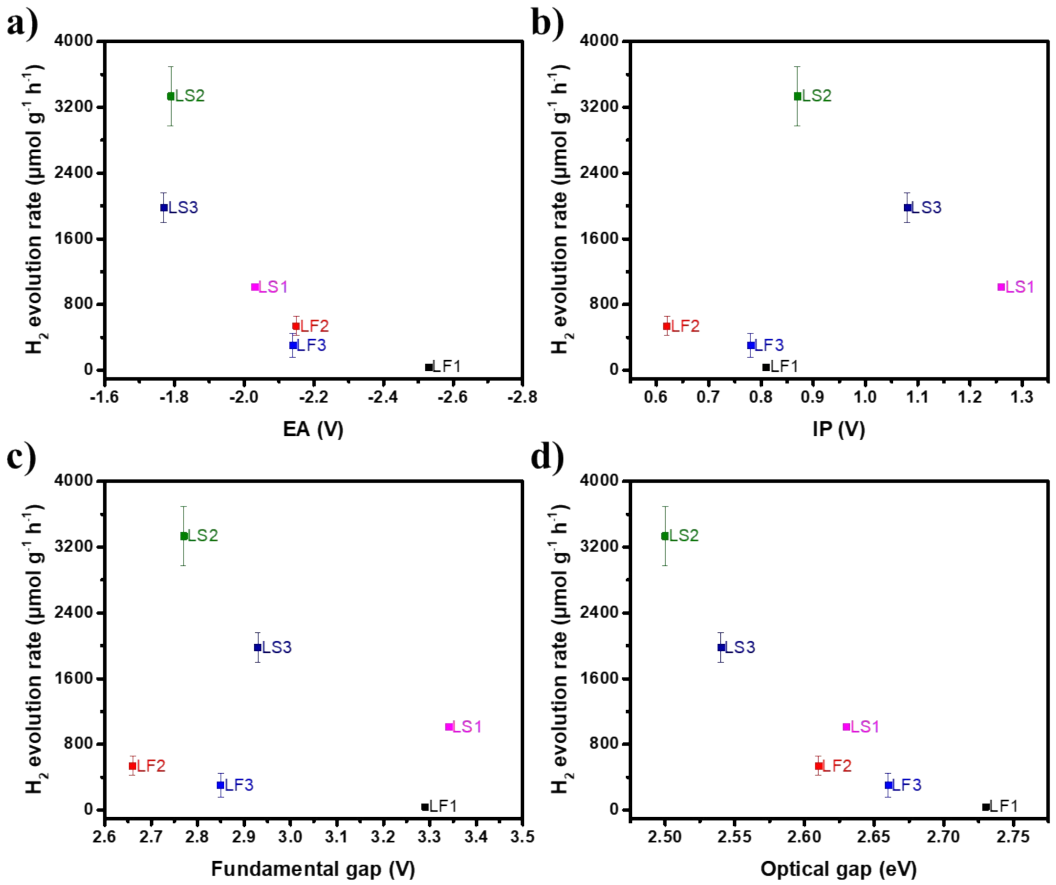

Fig. S18: Comparison of the hydrogen evolution rates to a) EA, b) IP, c) fundamental gap (IP-EA) and d) optical gap of LS1-3 and LF1-3.

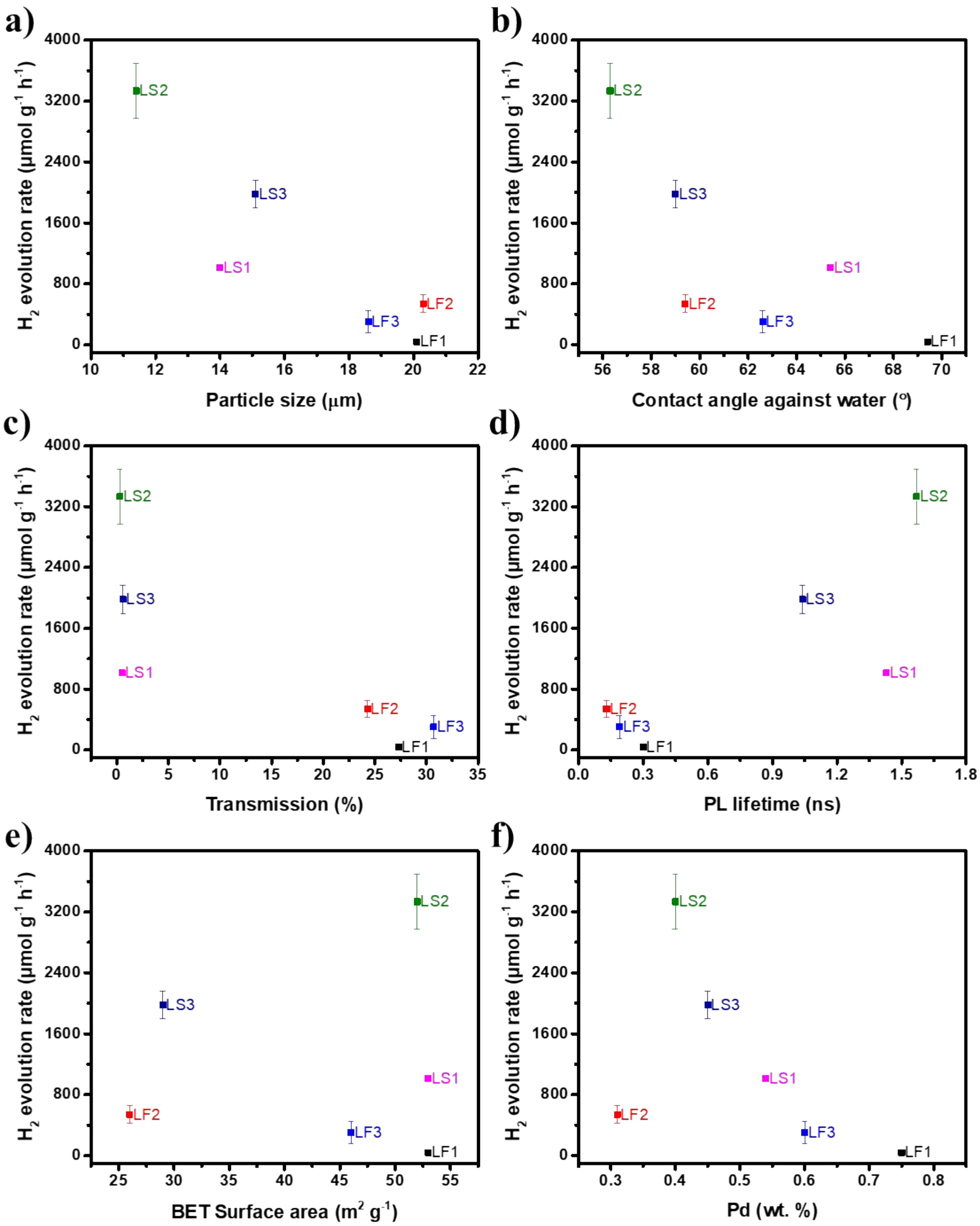

Fig. S19: Comparison of the hydrogen evolution rates to a) particle size, b) contact angle (against water), c) transmission, d) averaged PL lifetime, e) BET surface area (SA_{BET}, N_2) and f) residue Pd content of LS1-3 and LF1-3.

References

1. L. Turcani, E. Berardo and K. E. Jelfs, *J. Comput. Chem.*, 2018, **39**, 1931-1942.
2. S. Grimme, C. Bannwarth and P. Shushkov, *J. Chem. Theory Comput.*, 2017, **13**, 1989-2009.
3. C. Bannwarth, S. Ehlert and S. Grimme, *J. Chem. Theory Comput.*, 2019, **15**, 1652-1671.
4. A. D. Becke, *J. Chem. Phys.*, 1993, **98**, 5648-5652.
5. P. J. Stephens, F. J. Devlin, C. F. Chabalowski and M. J. Frisch, *J. Phys. Chem.*, 1994, **98**, 11623-11627.
6. A. Schäfer, H. Horn and R. Ahlrichs, *J. Chem. Phys.*, 1992, **97**, 2571-2577.
7. J. Gauss, *J. Chem. Phys.*, 1993, **99**, 3629-3643.
8. A. Klamt and G. Schüürmann, *J. Chem. Soc., Perkin Trans. 2*, 1993, **2**, 799-805.
9. A. Schäfer, A. Klamt, D. Sattel, J. C. W. Lohrenz and F. Eckert, *Phys. Chem. Chem. Phys.*, 2000, **2**, 2187-2193.
10. S. Grimme, J. Antony, S. Ehrlich and H. Krieg, *J. Chem. Phys.*, 2010, **132**, 154104.
11. Y. Bai, L. Wilbraham, B. J. Slater, M. A. Zwijnenburg, R. S. Sprick and A. I. Cooper, *J. Am. Chem. Soc.*, 2019, **141**, 9063-9071.
12. M. Sachs, R. S. Sprick, D. Pearce, S. A. J. Hillman, A. Monti, A. A. Y. Guilbert, N. J. Brownbill, S. Dimitrov, X. Shi, F. Blanc, M. A. Zwijnenburg, J. Nelson, J. R. Durrant and A. I. Cooper, *Nat. Commun.*, 2018, **9**, 4968.
13. R. S. Sprick, Y. Bai, A. A. Y. Guilbert, M. Zbiri, C. M. Aitchison, L. Wilbraham, Y. Yan, D. J. Woods, M. A. Zwijnenburg and A. I. Cooper, *Chem. Mater.*, 2019, **31**, 305-313.
14. C. B. Meier, R. S. Sprick, A. Monti, P. Guiglion, J.-S. M. Lee, M. A. Zwijnenburg and A. I. Cooper, *Polymer*, 2017, **126**, 283-290.
15. C. Yang, B. C. Ma, L. Zhang, S. Lin, S. Ghasimi, K. Landfester, K. A. I. Zhang and X. Wang, *Angew. Chem. Int. Ed.*, 2016, **55**, 9202-9206.
16. S. Bi, Z.-A. Lan, S. Paasch, W. Zhang, Y. He, C. Zhang, F. Liu, D. Wu, X. Zhuang, E. Brunner, X. Wang and F. Zhang, *Adv. Funct. Mater.*, 2017, **27**, 1703146.
17. C. Shu, C. Han, X. Yang, C. Zhang, Y. Chen, S. Ren, F. Wang, F. Huang and J.-X. Jiang, *Adv. Mater.*, 2021, **33**, 2008498.
18. L. Li, Z. Cai, Q. Wu, W.-Y. Lo, N. Zhang, L. X. Chen and L. Yu, *J. Am. Chem. Soc.*, 2016, **138**, 7681-7686.
19. D. Zeng, W. Xu, W.-J. Ong, J. Xu, H. Ren, Y. Chen, H. Zheng and D.-L. Peng, *Appl. Catal. B-Environ.*, 2018, **221**, 47-55.
20. A. R. Jones, *Prog. Energy Combust. Sci.*, 1999, **25**, 1-53.